# 2-kpc scale CO(3-2) imaging of a strongly-lensed wet-merger at $z\sim0.65$

**P.I.: T. K. Daisy Leung**

**Star formation modes and molecular gas dynamics beyond the local universe**

Tremendous progress has been made towards our understanding of the high-$z$ universe over the past two decades (see recent reviews by Carilli & Walter 2013; Madau & Dickinson 2014; Casey et al. 2014). These studies suggest that the elevated star formation rates (SFRs) and specific SFRs observed in galaxies at the peak epoch of star formation ($1\lesssim z\lesssim3$) are primarily driven by their increased in molecular gas mass fractions and star formation efficiencies (SFEs) compared to local galaxies, and that star formation in these early systems can be grossly categorised into two dominant modes – quiescent mode in disk-like galaxies versus starburst mode in commonly merger-driven starburst galaxies and quasar host galaxies (e.g. Sargent et al. 2012). The systematically enhanced molecular gas fractions observed in high-$z$ galaxy populations imply that their star-forming clumps are expected to be larger in size due to larger internal turbulence compared to nearby galaxies. Indeed, recent studies have found gas clumps on the order of $\sim1-2$ kpc scales at $z\sim1$–2 (e.g. Genzel et al. 2011; Swinbank et al. 2012a,b), providing direct evidence that the interstellar medium (ISM) conditions of galaxies evolve as a function of cosmic time. This highlights the importance of resolving gas dynamics of galaxies on these scales and at various epochs in order to investigate the mechanisms and physical processes responsible for the two star formation modes and for causing the steep decline in the cosmic SFR density since $z\sim1.5$ (e.g. Lagos et al. 2011; Popping et al. 2012).

While studies using spatially resolved CO observations in local ultra-luminous IR galaxies (ULIRGs) and their high-$z$ analogues ($z\gtrsim1$ starburst systems) have enabled a better understanding of the gas properties of mergers at these epochs (e.g. Carilli et al. 2010; Engel et al. 2010; Bothwell et al. 2010; Riechers et al. 2011; Ivison et al. 2011), the gas properties such as excitation, distribution, and dynamics of mergers at intermediate redshift ($0.6\lesssim z\lesssim1$) — the epoch where the star formation history is steeply rising — remain largely unknown due to the lack of spatially resolved CO observations at these redshifts. Thus, to understand of the role of mergers throughout cosmic history and to obtain a coherent picture connecting high-$z$ populations to present-day galaxies, it is vital to carry out detailed studies of the gas kinematics and dynamics at intermediate redshift.

We have recently imaged CO(2-1) line emission in the strongly-lensed quasar host galaxy RXJ 1131−1231 (hereafter RX1131) at $z\sim0.65$ with the PdBI/NOEMA (Fig. 1; Leung et al. 2016). We here propose to image **CO(3-2)** at higher resolution using the **A+C array configuration**. By combining the magnification provided by gravitational lensing with the improved spatial resolution and sensitivity of NOEMA, the proposed resolution of ∼0.6" corresponding to a physical scale of ∼1.8 kpc in the source plane at the target redshift will allow us to study the internal gas dynamics and distribution down to the physical scales of high-$z$ star-forming clumps **in only 1.5 hours on source**. Since our target is currently the only source with spatially resolved CO imaging at intermediate redshift with existing multi-wavelength analysis spanning rest-frame UV-to-radio, obtaining the proposed observations will enable, for the first time, a kpc-scale characterisation of the gas, dust, and stellar populations in a quasar host galaxy and merger at intermediate redshift.

**Unique Nature of our target RXJ 1131−1231**

RXJ1131 is a quadruply-imaged optical quasar (bright knots in Fig. 1d) with its host galaxy being lensed into a partial Einstein ring (Fig. 1d & Fig. 2; Sluse et al. 2003). Source-plane reconstruction of an optical image indicates that the host galaxy displays a disk-like morphology, with a companion galaxy located at ∼2.4 kpc away (Fig. 1f; Claeskens et al. 2006; Brewer & Lewis 2008). We have recently confirmed that both galaxies are at the same redshift by detecting their CO(2-1) emission and decomposing their gas distribution via our $uv$-plane lens modeling of the NOEMA CO(2-1) data in velocity-space (Fig. 1c & e; Leung et al. 2016), finding a gas mass of $M_{\rm gas}\sim1.4\times10^{10}\,M_\odot$ for RXJ1131. Our dynamical lens modelling shows that the asymmetry in the double-horned line profile (Fig. 1a) is mainly a result of differential lensing, where the magnification factor varies from ∼3 to ∼9 across different kinematic components. The intrinsically symmetric double-horned line profile of RXJ1131 (Fig. 1c) together with its source-plane velocity gradient and rotation profile (Fig. 2) suggest that RX1131 is an extended disk of $\gtrsim6$ kpc in radius. We find a lensing-corrected IR luminosity of $1.5\times10^{12}\,L_\odot$ based on our spectral energy distribution (SED) modelling (Fig. 3), indicating that RXJ1131 is a ULIRG with a SFR $\sim120\,M_\odot$ yr$^{-1}$. We also find that RXJ1131

contains a baryonic gas fraction of $f_{\rm mol} \sim 32\%$ that is higher than local galaxies but modest compared to $z \sim 2$ disk galaxies (Daddi et al. 2010).

Despite similar IR luminosity, CO linewidth and SFR found between RXJ1131 and other ULIRGs/high-$z$ starburst galaxies, its CO source size, gas depletion timescale and SFE are similar to those of nearby and high-$z$ disk galaxies rather than starburst systems. This suggests that the star formation in RXJ1131 mainly driven by global gravitational instabilities due to its high gas fraction rather than merger-induced gas accumulation, in contrast to local ULIRGs/mergers and high-$z$ starbursts. On the other hand, we find disturbed gas morphologies with velocity dispersion exceeding 400km s$^{-1}$ near the central region of RXJ1131 (Fig. 1e), but since the emission is only resolved over $\sim$2$-$3 beams at the resolution of our current data ($\sim$4.4"$\times$2"), it is impossible to quantify dispersions due to perturbations from its AGN, turbulence from interactions with its companion, and gravitational instability due to the huge gas reservoir.

**This proposal**

We propose to map CO(3-2) line emission in RXJ1131 which we have already detected with CARMA at moderate S/N and resolution ($\sim$3"). Based on scaling relations (Genzel et al. 2011), we expect clump size of $\sim$1.9 kpc in RXJ1131. Thus, the proposed resolution of $\sim$0.7" ($\sim$1.8 kpc in the source plane at $z \sim 0.65$) will enable us to derive $v_{\rm rot}/\sigma$ on this scale length, enabling us to quantify whether RXJ1131 is a rotation- or dispersion-dominated system, and to examine its internal dynamics by studying the spatial variations in $v_{\rm rot}/\sigma$. Previous studies have shown that resolutions corresponding to $\sim$1.7$-$2 kpc are sufficient to withstand beam smearing effect to extract rotation velocity and dispersion even at $z \sim 2$ (e.g. Newman et al. 2013; Genzel et al. 2014). The $v_{\rm rot}/\sigma$ ratio together with gas size and surface density will enable us to compute the theoretical Jeans length, which we will then use to determine the dynamical timescales of the star-forming clumps in RXJ1131 to examine its star-forming conditions and mechanisms. We will derive the rotation velocity by reconstructing the intrinsic gas distribution and velocity field using a similar approach as with our NOEMA CO(2-1) data (Fig. 2), but at much higher precision. This will enable us to derive reliable estimates on the rotation velocity, inclination angle, and dynamical mass by fitting disk models.

We will measure spatially resolved line ratios within RX1131 to gain insight into its gas excitation conditions. The molecular gas distribution, kinematics and line ratio variations will provide clues to the main driver of star formation in RXJ1131 (e.g. if the warmer gas is concentrated toward the central region of RX1131 like in nearby ULIRGs), how interactions with the companion influence the molecular gas in fueling its ongoing star formation and the central quasar, and how its gas excitation differs from other galaxy populations at different cosmic epochs. Additionally, we expect to detect continuum emission underlying CO(3-2) line at $\sim$5-10$\sigma$ significance based on our SED model and the observed image ratios at radio wavelengths. Hence, the proposed data will also allow us to place constraints on the spatially resolved "star formation law" at $z \sim 0.65$.

Given the rare lensing configuration and nature of our target, the proposed observations present an excellent opportunity to investigate the molecular gas excitation, kinematic and dynamical state of a distant quasar host galaxy, allowing us to investigate how physical parameters, e.g. stellar mass, dust temperature, SFR, SFE, and morphology, which have been investigated at both nearby and $z \gtrsim 1$ galaxies, vary at intermediate redshift depending on the molecular gas properties.

**Technical justification** We propose to observe CO(3-2) emission in RXJ1131 at $z_{\rm CO} = 0.6537$ at the redshifted line frequency of 209.10443 GHz ($\nu_{\rm rest} = 345.79599$ GHz) using the A+C array configurations. Given the spatial extent the quasar host galaxy ($\sim$3.8" in diameter), we request C-array observations to provide short spacings to maximize the sensitivity and $uv$ coverage for lens modelling, and to ensure that diffuse lensed emission on $\gtrsim$0.3" scale is not resolved out. We estimate the expected source size based on the most extended kinematic component in our dynamical lens model of the CO(2-1) data, which takes into account the asymmetric line emission and spatial extent across different velocity bins (arising due to differential lensing). We therefore expect the source to be resolved over $\sim$10 beams at the proposed angular resolution of $\sim$0.66". We compute the expected CO(3-2) line strength based on our CARMA CO(3-2) line flux of $I = 35.7$ Jy km s$^{-1}$ and line FWHM of $\sim$700 km s$^{-1}$. To obtain sufficient S/N for dynamical lens modelling over 7$-$10 velocity bins, we require a 10$\sigma$ detection of $\sigma = 1.35$ mJy beam$^{-1}$ per 100 km s$^{-1}$ bin, **requiring only $\sim$1.5 hours on source** (and 2.4 hours including overheads) with 8 antennas. We note that the requested sensitivity will correspond to S/N>10 for channels with spatially less extended emission, which are also found to have lower magnification factors (and thus lower apparent flux density).

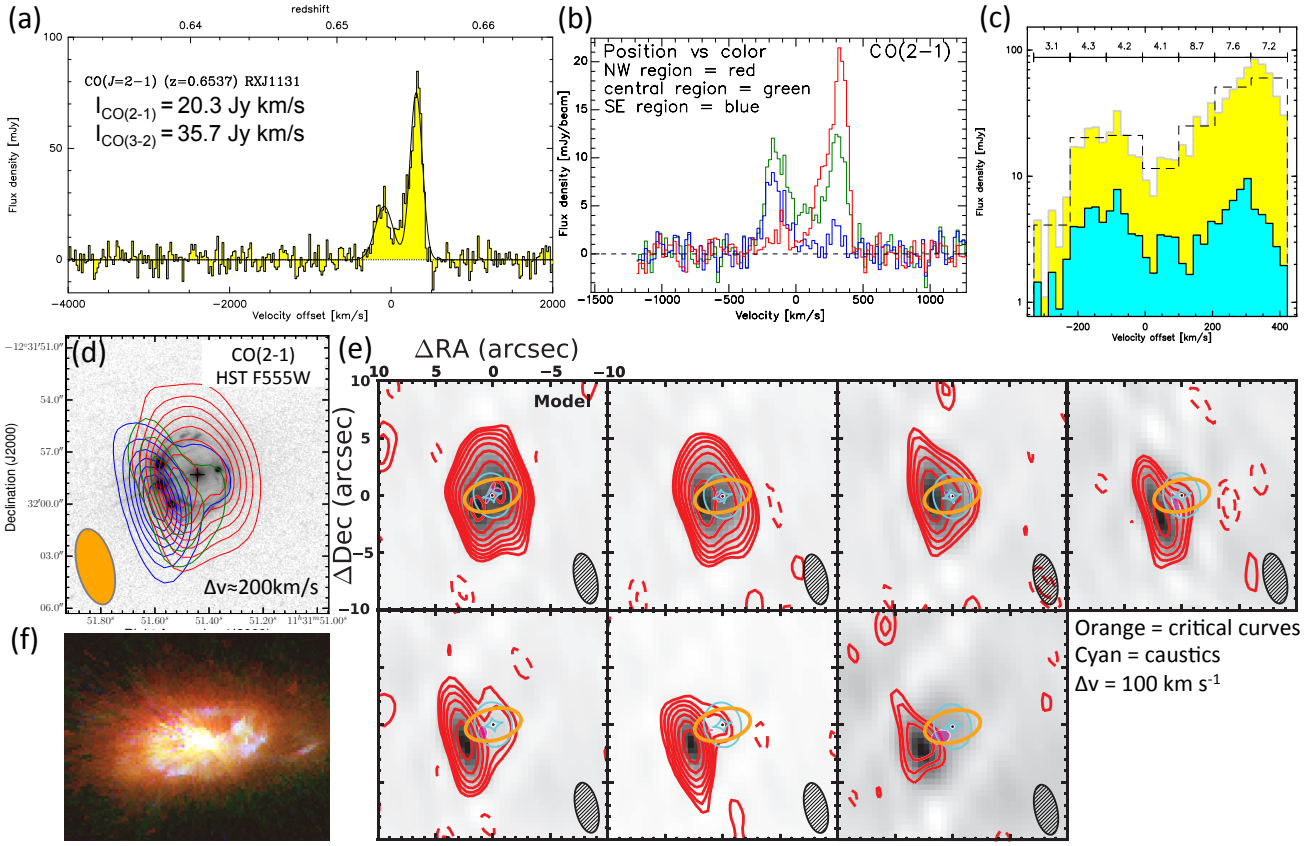


Figure 1: **Recent CO(2-1) observations from NOEMA and *uv*-plane lens modelling of RXJ1131 (Leung et al. 2016).** *(a):* Asymmetric double-horned (apparent) line profile observed towards our target. *(b):* Spectra taken at three locations along the strongest velocity gradient, demonstrating differential lensing of different kinematic components. *(c):* Full resolution spectrum (yellow; same as panel *a* but shown on log-scale) and the seven channels (dashed) used for lens modeling. Using the magnification factors indicated above the model channels, we recover an intrinsically symmetric "twin peak" profile (blue) as expected for a rotating disk. *(d):* Observed spatial variations across different velocity components due to differential lensing, as shown by the red (redshifted), green (line center), and blue (blueshifted) contours overlaid on an HST image of the rest-frame optical emission of the stellar light and AGN. *(e):* Channel maps of the CO emission (red) overlaid on our best-fit *uv*-plane lens models (grayscale). The reconstructed source morphology (magenta ellipses) is suggestive of a "disk", consistent with that in the optical *(f)*. We propose to observe CO(3-2) line in RXJ1131 at the spatial scales of individual star-forming clumps (∼1.9 kpc) to investigate its molecular gas excitation, kinematic and dynamical state and how physical properties, e.g. stellar mass, dust temperature, SFR, SFE, morphology, clumpiness, vary at intermediate redshift depending on the molecular gas conditions.

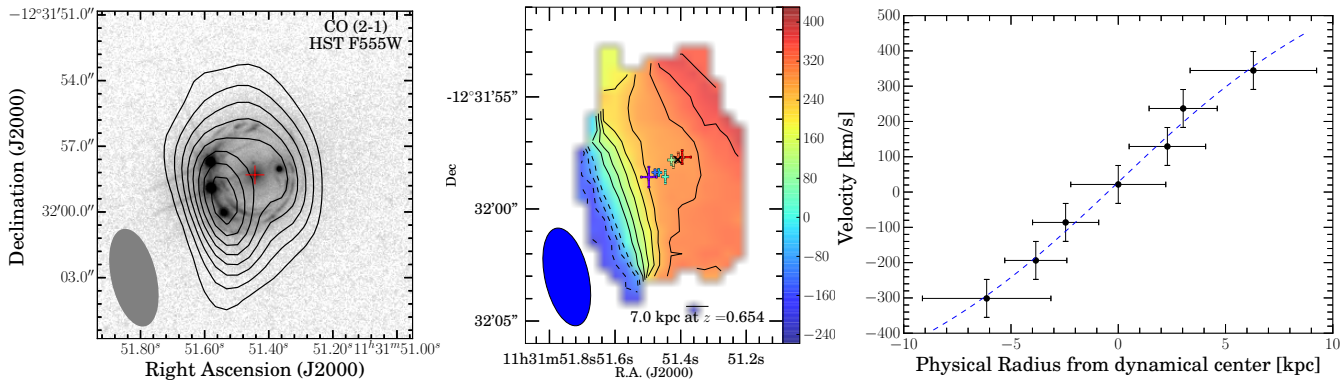


Figure 2: **Gas morphology and dynamical constraints from lens modelling of our NOEMA CO(2-1) data.** *Left:* Extended CO emission overlaid on an optical image. *Middle:* Source-plane positions of different kinematic components have been reconstructed from our NOEMA data using a velocity-space lens modelling approach in the *uv*-plane, as indicated by color markers atop the observed first moment map. The spectrally resolved lensed emission allows us to probe dynamical structures on spatial scales smaller the synthesis beam. *Right:* Position-velocity diagram along the source-plane major axis at PA = 121°. Dashed line shows the best-fit rotation curve. Our dynamical modelling is currently limited by the poorly resolved rotation profile in the central ∼2kpc. At the proposed resolution, we will be able to obtain more accurate lens modelling of different kinematic components, and on smaller spatial scales, allowing us to resolve the steep central gradient of the rotation curve. This will enable us to derive more reliable estimates on the rotation velocity, inclination angle, and dynamical mass for this intermediate-$z$ quasar host galaxy.

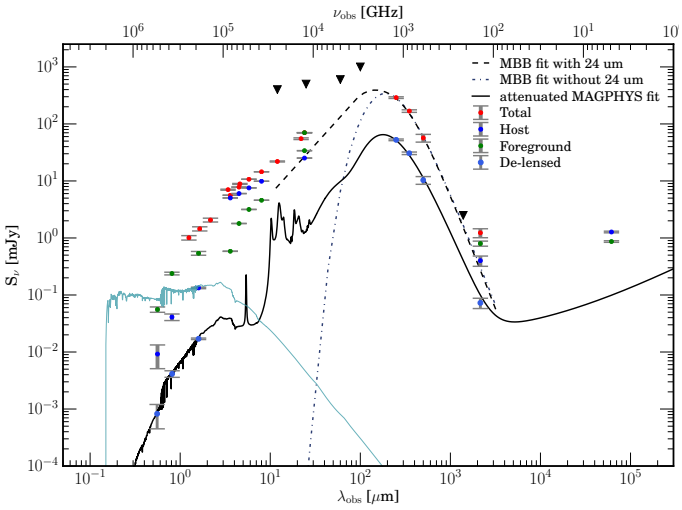


Figure 3: **Multi-wavelength photometry and SED models (Leung et al. 2016).** We have deblended rest-frame UV-to-radio photometry in our target (blue markers) from its foreground lensing galaxy. The dashed and dashed-dotted lines correspond to the best-fit dust SED models (uncorrected for lensing) and the black line corresponds to the best-fit full SED model (corrected for lensing). We estimate a continuum flux of ∼1.5−3.4 mJy by extrapolating SED models to the proposed frequency. We thus expect to detect continuum emission underlying CO(3-2) line at ∼5-10$\sigma$ significance. This will allow us to place constraints on the spatially resolved "star formation law" to investigate how the star formation mode of this intermediate-$z$ quasar host galaxy compares to those at low and high redshift.

**References** • Bothwell et al. 2010, MNRAS, 405, 219 • Brewer et al. 2008, MNRAS, 390, 39 • Carilli et al. 2010, ApJ, 714, 1407 • Carilli et al. 2013, ARA&A, 51, 105 • Casey et al. 2014, Phys. Rep., 541, 45 • Claeskens et al. 2006, A&A, 451, 865 • Daddi et al. 2010, ApJ, 713, 686 • Engel et al. 2010, ApJ, 724, 233 • Genzel et al. 2014, ApJ, 785, 75 • Genzel et al. 2011, ApJ, 733, 101 • Ivison et al. 2011, MNRAS, 412, 1913 • Lagos et al. 2011, MNRAS, 418, 1649 • Leung et al. 2016, ApJ, submitted • Madau et al. 2014, ARA&A, 52, 415 • Newman et al. 2013, ApJ, 767, 104 • Popping et al. 2012, MNRAS, 425, 2386 • Riechers et al. 2011, ApJ, 733, L11 • Sargent et al. 2012, ApJ, 747, L31 • Sluse et al. 2003, A&A, 406, L43 • Swinbank et al. 2012a, ApJ, 760, 130 • Swinbank et al. 2012b, MNRAS, 426, 935